

C: Surfaces, Interfaces, Porous Materials, and Catalysis

In Silico Optimization of Organic-Inorganic Hybrid Perovskites for Photocatalytic Hydrogen Evolution Reaction in Acidic Solution

Lu Wang, William A. Goddard, Tao Cheng, Hai Xiao, and Youyong Li

J. Phys. Chem. C, **Just Accepted Manuscript** • DOI: 10.1021/acs.jpcc.8b07380 • Publication Date (Web): 04 Aug 2018

Downloaded from <http://pubs.acs.org> on August 6, 2018

Just Accepted

“Just Accepted” manuscripts have been peer-reviewed and accepted for publication. They are posted online prior to technical editing, formatting for publication and author proofing. The American Chemical Society provides “Just Accepted” as a service to the research community to expedite the dissemination of scientific material as soon as possible after acceptance. “Just Accepted” manuscripts appear in full in PDF format accompanied by an HTML abstract. “Just Accepted” manuscripts have been fully peer reviewed, but should not be considered the official version of record. They are citable by the Digital Object Identifier (DOI®). “Just Accepted” is an optional service offered to authors. Therefore, the “Just Accepted” Web site may not include all articles that will be published in the journal. After a manuscript is technically edited and formatted, it will be removed from the “Just Accepted” Web site and published as an ASAP article. Note that technical editing may introduce minor changes to the manuscript text and/or graphics which could affect content, and all legal disclaimers and ethical guidelines that apply to the journal pertain. ACS cannot be held responsible for errors or consequences arising from the use of information contained in these “Just Accepted” manuscripts.



ACS Publications

is published by the American Chemical Society, 1155 Sixteenth Street N.W., Washington, DC 20036

Published by American Chemical Society. Copyright © American Chemical Society. However, no copyright claim is made to original U.S. Government works, or works produced by employees of any Commonwealth realm Crown government in the course of their duties.

In silico Optimization of Organic-inorganic Hybrid Perovskites for Photocatalytic Hydrogen Evolution Reaction in Acidic Solution

Lu Wang^{†,‡}, William A. Goddard III^{*,‡,§}, Tao Cheng^{‡,§}, Hai Xiao^{‡,§}, and Youyong Li^{*,†}

[†] Institute of Functional Nano & Soft Materials (FUNSOM), Jiangsu Key Laboratory for Carbon-Based Functional Materials & Devices, Soochow University, Suzhou, Jiangsu 215123, China

[‡] Materials and Process Simulation Center (MSC), California Institute of Technology, Pasadena, California 91125, United States

[§] Joint Center for Artificial Photosynthesis (JCAP), California Institute of Technology, Pasadena, California 91125, United States

ABSTRACT

We previously reported the atomistic reaction mechanism for the photocatalytic hydrogen evolution reaction (HER) on the $\text{CH}_3\text{NH}_3\text{PbI}_3$ organic-inorganic hybrid perovskites based on quantum mechanics (QM) calculations of the transition state barriers, including several layers of explicit acidic solvent. Here we extend these studies using *in silico* optimization to discover additional promising photocatalysts. We consider replacing

- Pb with Sn,
- I with Br, and
- CH_3NH_3 cation with several organic cations, including $\text{NH}_2(\text{CH})\text{NH}_2$ cation

as the photocatalyst for HER. We compared the activation barriers and reaction energies for each case. In our previous studies, we found that both H atoms of the H_2 product are extracted from surface organic cations with protons from the solution migrating along Grotthuss water chains to replace the H of the organic cations. This two-step reaction mechanism involves formation of an intermediate lead hydride bond, with the lead atoms and the surface organic cations both playing essential roles. Among the perovskites investigated here, we predict that $\text{NH}_2(\text{CH})\text{NH}_2\text{PbI}_3$ exhibits the best HER performance with a predicted 10-fold improvement in the reaction rate compared to $\text{CH}_3\text{NH}_3\text{PbI}_3$. We also suggest that the lead-free tin-iodide perovskites might exhibit a rate comparable to that of lead-iodide perovskites with the same organic cations. However, replacing iodine by bromine significantly increases the activation barrier. We find for these lead-iodide perovskites, the increased proton affinity of the surface organic cations enhances the photocatalytic efficiency, with $\text{NH}_2(\text{CH})\text{NH}_2$ the best case examined.

KEYWORDS

photocatalytic reaction mechanism, quantum mechanics, perovskite, density functional theory

Photochemical generation of H₂ provides a potentially renewable process to address the energy and environmental issues without producing pollution. In early developments, TiO₂ photocatalysts loaded with small amounts of Pt or Rh nanoparticles were co-catalysts to generate H₂ by splitting water under the UV light.^{1,2} Later, other metal oxides and metal sulfides, such as CdS and WO₃, were examined as heterogeneous photocatalysts.^{3,4} Moreover, such two-dimensional nanomaterials as ZnSe, g-C₃N₄, and transition metal chalcogenides have shown promise as efficient photocatalysts with a high specific surface area and long electron/hole diffusion distances.⁵⁻⁷ More recently, organic-inorganic hybrid perovskites, such as CH₃NH₃PbI₃ have taken a dominant position in the photovoltaic field.^{8,9} They can be fabricated by a simple, easy solution process and comprise earth-abundant elements, making them low-cost. Their outstanding properties include optimal band gaps (1.5 eV-2.0 eV), low exciton binding energy,¹⁰ and long carrier lifetime,¹¹ provide promising routes to efficiently utilize sunlight for water splitting. The power conversion efficiency for the organic-inorganic perovskites is already over 20%, suggesting them as potential future solar cell absorption materials.

The general formula of these organic-inorganic perovskites is ABX₃, where A is the organic cation (CH₃NH₃⁺, NH₃NH₂⁺, etc.), B can be a group IV di-cation such as Pb or Sn, and X can be a halogen such as Cl, Br, I. The electronic properties of these perovskites depend on their combinations, with many mixtures successfully synthesized to find improved structural stability, reproducibility, and high efficiency.^{12,13} Recently, CH₃NH₃PbI₃ perovskite was shown experimentally to act as a photocatalyst for H₂ generation in aqueous HI solution.^{14,15} Under visible light irradiation, CH₃NH₃PbI₃ powder efficiently catalyzes formation of H₂ and I₃⁻ in experiments. We recently reported the reaction mechanism for this photocatalysis, discovering a novel two-step Pb-activated amine-assisted (PbAAA) reaction mechanism for hydrogen evolution reaction (HER) on the CH₃NH₃PbI₃ surface.¹⁶ Thus, in addition to serving as a photo-absorber for visible light, the CH₃NH₃PbI₃ perovskite serves as a catalyst reductant for the HER with the lead atoms and the surface organic cations both playing critical roles. We found that both H of the H₂ product are extracted from surface CH₃NH₃⁺ cations, while their protons are replaced from the solution through migration along Grotthuss water chains.

Here we report *in silico* studies to discover potential improved photocatalysts. To do this we first used the two-step PbAAA reaction mechanism to examine whether the other organic cations perovskites might improve the photocatalytic efficiency. Second, we considered tin iodide perovskite as a potential lead-free photocatalyst for HER. Third, we examined Br replacement of I as the photocatalyst for H₂ production. We used the same methodology (Quantum Mechanics, QM) at the PBE-D3 level with three layers of explicit solvent to determine the reaction barriers for the photocatalytic HER reaction for five kinds of organic cations, for tin iodide perovskite, and for lead bromide perovskite, respectively.

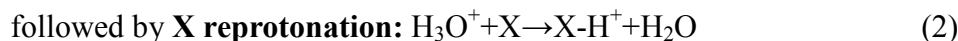
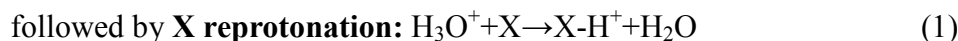
Here, we use the 2×2 supercell of the (010) surface of orthorhombic $\text{CH}_3\text{NH}_3\text{PbI}_3$ as the initial structure to replace only one surface CH_3NH_3^+ cation by the other organic cations as a fast way to discover promising organics. For the most promising cases, we might later consider full crystals of the new organic cations or maybe a mixed system if the new organic cation prefers the surface. We derived the surfaces for lead bromide perovskite of $\text{CH}_3\text{NH}_3\text{PbBr}_3$ and the tin iodide perovskite of $\text{CH}_3\text{NH}_3\text{SnI}_3$ from their orthorhombic crystal structures. The construction of the electrode-electrolyte interface is the same as in our previous study, with 64 H_2O forming three layers over the 2 by 2 supercell.¹⁶ To simulate the acidic environment during the HER reaction, we included three HI molecules in the solvent structure for iodide-based perovskites, and three HBr molecules for bromide-based perovskites. After structural relaxation, the three HI (or HBr) molecules dissociate into three I^- (or Br^-) ions plus three H_3O^+ molecules in the solution. To describe the photoexcited state, we added two potassium atoms to populate the conduction band of the perovskite. The whole system is fully relaxed with only the bottom layer fixed.

All calculations were performed using the Vienna Ab initio Simulation Package (VASP)^{17,18} using the projector augmented wave (PAW) method to account for core-valence interactions.^{19,20} The Perdew-Burke-Ernzerhof (PBE) functional²¹ of density functional theory (DFT) including the D3 van der Waals correction was used.²² The kinetic energy cutoff for plane wave expansions was set to 350 eV, and reciprocal space was sampled using the Γ -point scheme. We applied Gaussian smearing using a small width of 0.05 eV. Transition state (TS) searches were conducted using the climbing image nudged elastic band (CI-NEB) method to generate the reaction path and the transition state structure.²³ All initial state (IS) and final state (FS) geometries were converged to within 5×10^{-2} eV/Å for maximal components of forces, and the forces on TS structures were converged to 0.1 eV/Å.

We examined five different organic cations to replace one CH_3NH_3^+ cation on the $\text{CH}_3\text{NH}_3\text{PbI}_3$ surface: $\text{C}_2\text{H}_5\text{NH}_3^+$, $(\text{CH}_3)_2\text{NH}_2^+$, NH_3NH_2^+ , NH_4^+ and $\text{NH}_2(\text{CH})\text{NH}_2^+$, which are popular cations for organic-inorganic hybrid perovskites. Compared to the size of the CH_3NH_3^+ cation (radius of 217 pm), the effective radii of $\text{C}_2\text{H}_5\text{NH}_3^+$, $(\text{CH}_3)_2\text{NH}_2^+$ and $\text{NH}_2(\text{CH})\text{NH}_2^+$ are larger with 274 pm, 272 pm, and 253 pm, respectively. The size of the NH_3NH_2^+ cation is the same as CH_3NH_3^+ (217 pm), and the effective radius of the NH_4^+ cation is the smallest with 146 pm.²⁴ The optimized surface structures are shown in Fig. 1. After structural optimizations, the orientations of the organic cations on the surface partition into two groups. One group [NH_3NH_2^+ , $(\text{CH}_3)_2\text{NH}_2^+$ and NH_4^+] leads to optimum orientations with the amine end upwards to form a hydrogen bond with an H_2O in the solution, while the other group [CH_3NH_3^+ , $\text{NH}_2(\text{CH})\text{NH}_2^+$ and $\text{C}_2\text{H}_5\text{NH}_3^+$] prefers downward orientations to form a hydrogen bond with an I atom in the PbI layer. During the reactions, these groups can flip.

Taking the doped organic cation as the active site for the HER reaction, we find the same two-step PbAAA reaction mechanism for each case. Denoting the organic cations as X-H^+ and the neutral organic molecule after losing one H^+ as X, the PbAAA reaction pathway for H_2 generation in acidic HI solvent can be written as:





9 This two-step HER reaction process on the $\text{CH}_3\text{NH}_3\text{PbI}_3$ surface, doped with one $\text{NH}_2(\text{CH})\text{NH}_2^+$
10 cation is shown in Fig. 2(a) as the representative with the initial structure, intermediate structure,
11 and final structure. The activation barriers and reaction energies, together with the H-Pb bond
12 length in the intermediate structure for different organic lead iodide perovskites are summarized
13 in Table 1.
14

15 **Pb activation**: First the H in the X-H^+ migrates to the Pb in the PbI layer, forming PbH^-
16 hydride intermediate. Prior to bonding to the H, the Pb had four equal Pb-I bonds (~ 3.2 Å) in the
17 PbI_2 plane, each formally involving transfer of $\frac{1}{2}$ electron from Pb to I. Forming the Pb-H bond
18 requires one sp hybrid on the Pb to bond to the H, leaving only one electron to share with the
19 four I in the PbI_2 plane. The result is that, in all the cases, two of the Pb-I bonds increase their
20 bond length to 3.7 Å, while the other two Pb-I bonds remain at 3.2 Å.
21

22 **First reprotonation**: After the H migrates from X-H^+ cation to Pb, leaving behind a neutral
23 X molecule, one H^+ transfers through a Grotthuss chain from the solution to the X molecule to
24 form a new X-H^+ cation.²⁵ Here, by consuming one proton from the solution and two electrons,
25 the **smallest activation barrier** to form the intermediate state of PbH^- hydride **is found for**
26 **$\text{NH}_2(\text{CH})\text{NH}_2^+$** with 0.97 eV, which also leads to the largest reaction energy of -1.83 eV. The
27 decreased activation barrier likely arises from the conjugation in $\text{NH}_2(\text{CH})\text{NH}_2^+$, with
28 delocalized electrons to facilitate the dehydrogenation of H^+ from $-\text{NH}_2^+$ to form PbH^- hydride.
29

30 **Hydrogen Evolution step**: Starting from the intermediate PbH^- hydride with a Pb-H bond
31 distance of 1.963 Å (taking $\text{NH}_2(\text{CH})\text{NH}_2^+$ as an example), another H^+ migrates from a
32 $\text{NH}_2(\text{CH})\text{NH}_2^+$ to react with PbH^- to generate H_2 , while regenerating the PbI_4 complex. This
33 energy barrier is 0.27 eV with the reaction energy decreasing by 2.29 eV.
34

35 **Second reprotonation**: A second proton from solution transfers through a Grotthuss chain
36 to reprotonate the neutral $\text{NH}_2(\text{CH})\text{NH}$ molecule to form a new $\text{NH}_2(\text{CH})\text{NH}_2^+$ cation.
37

38 Thus, over the whole photocatalytic HER reaction process, the surface structure with one
39 $\text{NH}_2(\text{CH})\text{NH}_2^+$ cation releases a total energy of 4.12 eV by consuming two electrons and two
40 protons. This is larger than that for the other doping cations, making $\text{NH}_2(\text{CH})\text{NH}_2\text{PbI}_3$ as the
41 most promising new photocatalyst for HER reaction. In table 1, we compare the predicted
42 barriers and energy release with the experimental gas phase proton affinities. We see that
43 $\text{NH}_2(\text{CH})\text{NH}_2^+$ possesses the largest proton affinity of 9.85 eV compared to the other molecules,
44 indicating that it would have the largest energy release, which is consistent with our simulation
45 results (energy release of 1.83 eV in the first step, larger than CH_3NH_3^+ with 1.35 eV). Thus, we
46 suggest that the organic perovskite with the amine cations possessing a larger proton affinity
47 likely exhibits a better HER performance.
48

49 **Lead Free**. In addition to doping of the surface cation, we also considered the lead-free
50
51
52
53
54
55

1
2
3 tin-based perovskite. The electronegativity of Sn (2.0) is similar to Pb (2.3) while the Sn-H bond
4 strength is larger, so we expected to a similar activation barrier for the formation of the
5 intermediate metal hydride bond, which is the rate-determining step for the HER reaction. Using
6 the same 2×2 supercell of the (010) surface of orthorhombic $\text{CH}_3\text{NH}_3\text{SnI}_3$ structure as the initial
7 surface configuration, we find that the energy barriers for the two-step HER reaction with the
8 lead-free $\text{CH}_3\text{NH}_3\text{SnI}_3$ surface are 1.16 eV and 0.23 eV, with a total reaction energy decrease of
9 3.35 eV, which are slightly less favorable than $\text{CH}_3\text{NH}_3\text{PbI}_3$. Extrapolating from our in silico
10 calculations, we suggest that **$\text{NH}_2(\text{CH})\text{NH}_2\text{SnI}_3$ perovskite** might be the most promising
11 **lead-free candidate**, with a reaction rate comparable to $\text{CH}_3\text{NH}_3\text{PbI}_3$.
12
13
14

15 **Iodine free.** We also considered the bromine-based perovskite as a candidate to replace I. We
16 examined the same 2×2 supercell of the (010) surface of orthorhombic $\text{CH}_3\text{NH}_3\text{PbBr}_3$ structure
17 as the initial surface configuration. The activation barriers for the two-step HER reaction on the
18 $\text{CH}_3\text{NH}_3\text{PbBr}_3$ surface are calculated to be 1.46 eV and 0.45 eV, respectively, which are much
19 higher than the results for $\text{CH}_3\text{NH}_3\text{PbI}_3$. To form the intermediate state of PbH^- hydride, two Pb-I
20 (or Pb-Br) bonds in the PbI (or PbBr) layer should be broken. The bond dissociation energy for
21 the Pb-Br bond is 2.57 eV, which is larger than the Pb-I bond of 2.01 eV, which may explain why
22 the Br case leads to a larger barrier. The reaction energy for the whole HER reaction process
23 decreases by 2.69 eV on the lead bromide perovskite surface, which is smaller than the results on
24 the lead iodide perovskites, especially on the second reaction step with 1.44 eV (compared to $>$
25 2.0 eV for the lead iodide perovskites). Therefore, based on our simulation results, the
26 **bromine-based perovskites are less promising** than the iodine-based perovskites as
27 photocatalysts for HER reaction to generate H_2 .
28
29
30
31
32

33 The activation barriers and reaction energies for the two-step HER reaction on the different
34 types of organic-inorganic hybrid perovskites are plotted in Fig. 2(b). We see clearly that
35 $\text{NH}_2(\text{CH})\text{NH}_2\text{PbI}_3$ (plotted in cyan color) is predicted to be the best new candidate for
36 photocatalytic HER. Using Eyring Transition state theory, we estimate that the rate of the HER
37 reaction on the surface $\text{NH}_2(\text{CH})\text{NH}_2^+$ site will be improved by a factor of 10 at 300 K compared
38 to the pristine $\text{CH}_3\text{NH}_3\text{PbI}_3$ surface.
39
40

41 Summarizing, we carried out QM calculations with three layers of explicit solvent for the
42 photocatalytic HER reaction on several modifications of the $\text{CH}_3\text{NH}_3\text{PbI}_3$ perovskite surface for
43 photochemical H_2 generation. For each case we find the same two-step metal-activated
44 amine-assisted reaction mechanism for HER. Comparing the various organic cations, we
45 estimate that $\text{NH}_2(\text{CH})\text{NH}_2^+$ cations on the surface may improve photocatalytic efficiency of the
46 HER reaction by decreasing the barrier of 0.11 eV, which at 300K would increase the rate by
47 10-fold. The bromine-based perovskites are less promising than the iodine-based perovskites as
48 the photocatalyst for the HER reaction.
49
50
51
52
53
54
55
56
57
58
59
60

AUTHOR INFORMATION

Corresponding Author

*yyli@suda.edu.cn

*wag@wag.caltech.edu; ORCID:0000-0003-0097-5716;

Notes

The authors declare no competing financial interests.

ACKNOWLEDGMENT

This work was supported by the National Key Research and Development Program of China (Grants 2018YFB0703900, 2017YFA0204800 and 2017YFB0701600), the National Natural Science Foundation of China (51761145013, 21673149). This research was also supported by the Joint Center for Artificial Photosynthesis, a DOE Energy Innovation Hub, supported through the Office of Science of the U.S. Department of Energy under Award No.DE-SC0004993. The work was carried out at National Supercomputer Center in Tianjin, and the calculations were performed on TianHe-1 (A). This project is also supported by the Fund for Collaborative Innovation Center of Suzhou Nano Science & Technology, the Priority Academic Program Development of Jiangsu Higher Education Institutions.

REFERENCES

- (1) Schrauzer, G. N.; Guth, T. D. Photocatalytic reactions. 1. Photolysis of water and photoreduction of nitrogen on titanium dioxide. *J. Am. Chem. Soc.* **1977**, *99*, 7189.
- (2) Fujishima, A.; Honda, K. Electrochemical photolysis of water at a semiconductor electrode. *Nature* **1972**, *238*, 37.
- (3) Aliev, A. S.; Mamedov, M. N.; Abbasov, M. T. Photoelectrochemical properties of TiO₂/CdS heterostructures. *Inorg. Mater.* **2009**, *45*, 965.
- (4) Kim, J.; Lee, C. W.; Choi, W. Platinized WO₃ as an environmental photocatalyst that generates OH radicals under visible light. *Environ. Sci. Technol.* **2010**, *44*, 6849.
- (5) Sun, Y.; Sun, Z.; Gao, S.; Cheng, H.; Liu, Q.; Piao, J.; Yao, T.; Wu, C.; Hu, S.; Wei, S.; Xie, Y. Fabrication of flexible and freestanding zinc chalcogenide single layers. *Nat. Comm.* **2012**, *3*, 1057.
- (6) Wang, X.; Maeda, K.; Thomas, A.; Takanabe, K.; Xin, G.; Carlsson, J. M.; Domen, K.; Antonietti, M. A metal-free polymeric photocatalyst for hydrogen production from water under visible light. *Nat. Mater.* **2008**, *8*, 76.
- (7) Chang, K.; Mei, Z.; Wang, T.; Kang, Q.; Ouyang, S.; Ye, J. MoS₂/graphene cocatalyst for efficient photocatalytic H₂ evolution under visible light irradiation. *ACS Nano* **2014**, *8*, 7078.
- (8) Burschka, J.; Pellet, N.; Moon, S.-J.; Humphry-Baker, R.; Gao, P.; Nazeeruddin, M. K.; Gratzel, M. Sequential deposition as a route to high-performance perovskite-sensitized solar cells. *Nature* **2013**, *499*, 316.

(9) Xing, G.; Mathews, N.; Sun, S.; Lim, S. S.; Lam, Y. M.; Grätzel, M.; Mhaisalkar, S.; Sum, T. C. Long-range balanced electron- and hole-transport lengths in organic-inorganic $\text{CH}_3\text{NH}_3\text{PbI}_3$. *Science* **2013**, *342*, 344.

(10) Miyata, A.; Mitioglu, A.; Plochocka, P.; Portugall, O.; Wang, J. T.-W.; Stranks, S. D.; Snaith, H. J.; Nicholas, R. J. Direct measurement of the exciton binding energy and effective masses for charge carriers in organic-inorganic tri-halide perovskites. *Nat. Phys.* **2015**, *11*, 582.

(11) Stranks, S. D.; Eperon, G. E.; Grancini, G.; Menelaou, C.; Alcocer, M. J. P.; Leijtens, T.; Herz, L. M.; Petrozza, A.; Snaith, H. J. Electron-hole diffusion lengths exceeding 1 micrometer in an organometal trihalide perovskite absorber. *Science* **2013**, *342*, 341.

(12) Jesper Jacobsson, T.; Correa-Baena, J.-P.; Pazoki, M.; Saliba, M.; Schenk, K.; Gratzel, M.; Hagfeldt, A. Exploration of the compositional space for mixed lead halogen perovskites for high efficiency solar cells. *Energy Environ. Sci.* **2016**, *9*, 1706.

(13) Saliba, M.; Matsui, T.; Seo, J.-Y.; Domanski, K.; Correa-Baena, J.-P.; Nazeeruddin, M. K.; Zakeeruddin, S. M.; Tress, W.; Abate, A.; Hagfeldt, A.; Gratzel, M. Cesium-containing triple cation perovskite solar cells: improved stability, reproducibility and high efficiency. *Energy Environ. Sci.* **2016**, *9*, 1989.

(14) Park, S.; Chang, W. J.; Lee, C. W.; Park, S.; Ahn, H.-Y.; Nam, K. T. Photocatalytic hydrogen generation from hydriodic acid using methylammonium lead iodide in dynamic equilibrium with aqueous solution. *Nat. Energy* **2016**, *2*, 16185.

(15) Yaqiang, W.; Peng, W.; Xianglin, Z.; Qianqian, Z.; Zeyan, W.; Yuanyuan, L.; Guizheng, Z.; Ying, D.; Myung Hwan, W.; Baibiao, H. Composite of $\text{CH}_3\text{NH}_3\text{PbI}_3$ with Reduced Graphene Oxide as a Highly Efficient and Stable Visible - Light Photocatalyst for Hydrogen Evolution in Aqueous HI Solution. *Adv. Mater.* **2018**, *30*, 1704342.

(16) Wang, L.; Xiao, H.; Cheng, T.; Li, Y.; Goddard, W. A. Pb-activated amine-assisted photocatalytic hydrogen evolution reaction on organic-inorganic perovskites. *J. Am. Chem. Soc.* **2018**, *140*, 1994.

(17) Kresse, G.; Furthmüller, J. Efficient iterative schemes for ab initio total-energy calculations using a plane-wave basis set. *Phys. Rev. B* **1996**, *54*, 11169.

(18) Kresse, G.; Hafner, J. Ab initio molecular dynamics for liquid metals. *Phys. Rev. B* **1993**, *47*, 558.

(19) Blöchl, P. E. Projector augmented-wave method. *Phys. Rev. B* **1994**, *50*, 17953.

(20) Kresse, G.; Joubert, D. From ultrasoft pseudopotentials to the projector augmented-wave method. *Phys. Rev. B* **1999**, *59*, 1758.

(21) Perdew, J. P.; Burke, K.; Ernzerhof, M. Generalized gradient approximation made simple. *Phys. Rev. Lett.* **1996**, *77*, 3865.

(22) Grimme, S.; Antony, J.; Ehrlich, S.; Krieg, H. A consistent and accurate ab initio parametrization of density functional dispersion correction (DFT-D) for the 94 elements H-Pu. *J. Chem. Phys.* **2010**, *132*, 154104.

(23) Henkelman, G.; Uberuaga, B. P.; Jónsson, H. A climbing image nudged elastic band method for finding saddle points and minimum energy paths. *J. Chem. Phys.* **2000**, *113*, 9901.

(24) Saparov, B.; Mitzi, D. B. Organic-inorganic perovskites: structural versatility for functional materials design. *Chem. Rev.* **2016**, *116*, 4558.

(25) Cheng, T.; Goddard, W. A.; An, Q.; Xiao, H.; Merinov, B.; Morozov, S. Mechanism and kinetics of the electrocatalytic reaction responsible for the high cost of hydrogen fuel cells. *Phys. Chem. Chem. Phys.* **2017**, *19*, 2666.

1
2
3 (26) Howard, S. T.; Platts, J. A.; Coogan, M. P. Relationships between basicity, structure, chemical shift
4 and the charge distribution in resonance-stabilized iminoamine. *J. Chem. Soc. Perkin Trans. 2*, **2002**, 899.

5
6 (27) Linstrom, P.; Mallard, W. Eds. *NIST Chemistry WebBook, NIST Standard Reference Database*
7 *Number 69*; National Institute of Standards and Technology: Gaithersburg, MD, 2003; <http://webbook.nist.gov>.
8
9
10
11
12
13
14
15
16
17
18
19
20
21
22
23
24
25
26
27
28
29
30
31
32
33
34
35
36
37
38
39
40
41
42
43
44
45
46
47
48
49
50
51
52
53
54
55
56
57
58
59
60

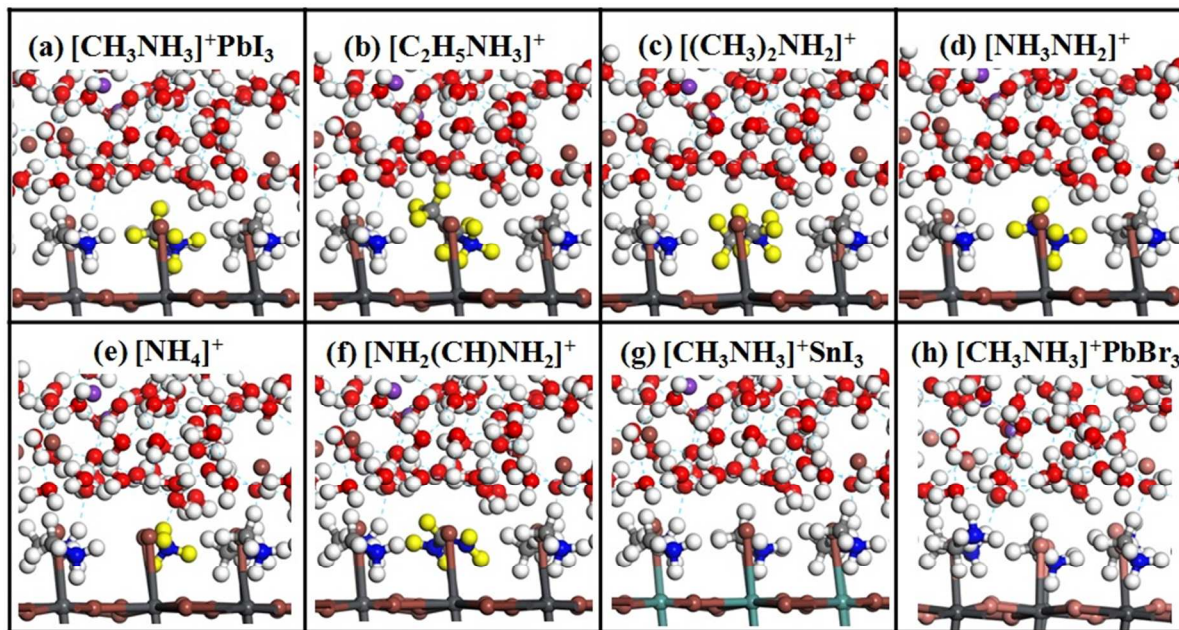


Figure 1. Optimized structures of (a) $\text{CH}_3\text{NH}_3\text{PbI}_3$ surface, with one surface CH_3NH_3^+ cation replaced by another organic cation (b) $\text{C}_2\text{H}_5\text{NH}_3^+$, (c) $\text{CH}_3\text{CH}_2\text{NH}_2^+$, (d) NH_3NH_2^+ , (e) NH_4^+ and (f) $\text{NH}_2(\text{CH})\text{NH}_2^+$, together with the structures of (g) $\text{CH}_3\text{NH}_3\text{SnI}_3$ and (h) $\text{CH}_3\text{NH}_3\text{PbBr}_3$ in the electrode-electrolyte interface models.

Table 1. Activation barriers (E_{a1} and E_{a2}) and reaction energies (E_{r1} and E_{r2}) for the two-step HER reaction on various organic-inorganic perovskites surfaces. Also shown is the experimental proton affinity (PA).^{26,27} We also include H-Pb (H-Sn) bond length in the intermediate structure. We see that $[\text{NH}_2(\text{CH})\text{NH}_2]\text{PbI}_3$ is predicted to be the best.

	E_{a1} (eV)	E_{r1} (eV)	H-Pb(Sn) bond length (Å)	E_{a2} (eV)	E_{r2} (eV)	PA (eV)
$[\text{CH}_3\text{NH}_3]^+\text{PbI}_3$	1.08	-1.35	1.970	0.08	-2.30	9.32
$[\text{C}_2\text{H}_5\text{NH}_3]^+$	1.05	-1.34	1.976	0.31	-2.03	9.45
$[(\text{CH}_3)_2\text{NH}_2]^+$	1.18	-1.45	1.981	0.14	-1.95	9.63
$[\text{NH}_3\text{NH}_2]^+$	1.10	-1.33	1.977	0.05	-2.31	8.84
$[\text{NH}_4]^+$	1.11	-1.46	1.968	0.13	-2.21	8.85
$[\text{NH}_2(\text{CH})\text{NH}_2]^+$	0.97	-1.83	1.963	0.27	-2.29	9.85
$[\text{CH}_3\text{NH}_3]^+\text{PbBr}_3$	1.46	-1.25	1.987	0.45	-1.44	--
$[\text{CH}_3\text{NH}_3]^+\text{SnI}_3$	1.16	-1.26	1.853	0.23	-2.09	--

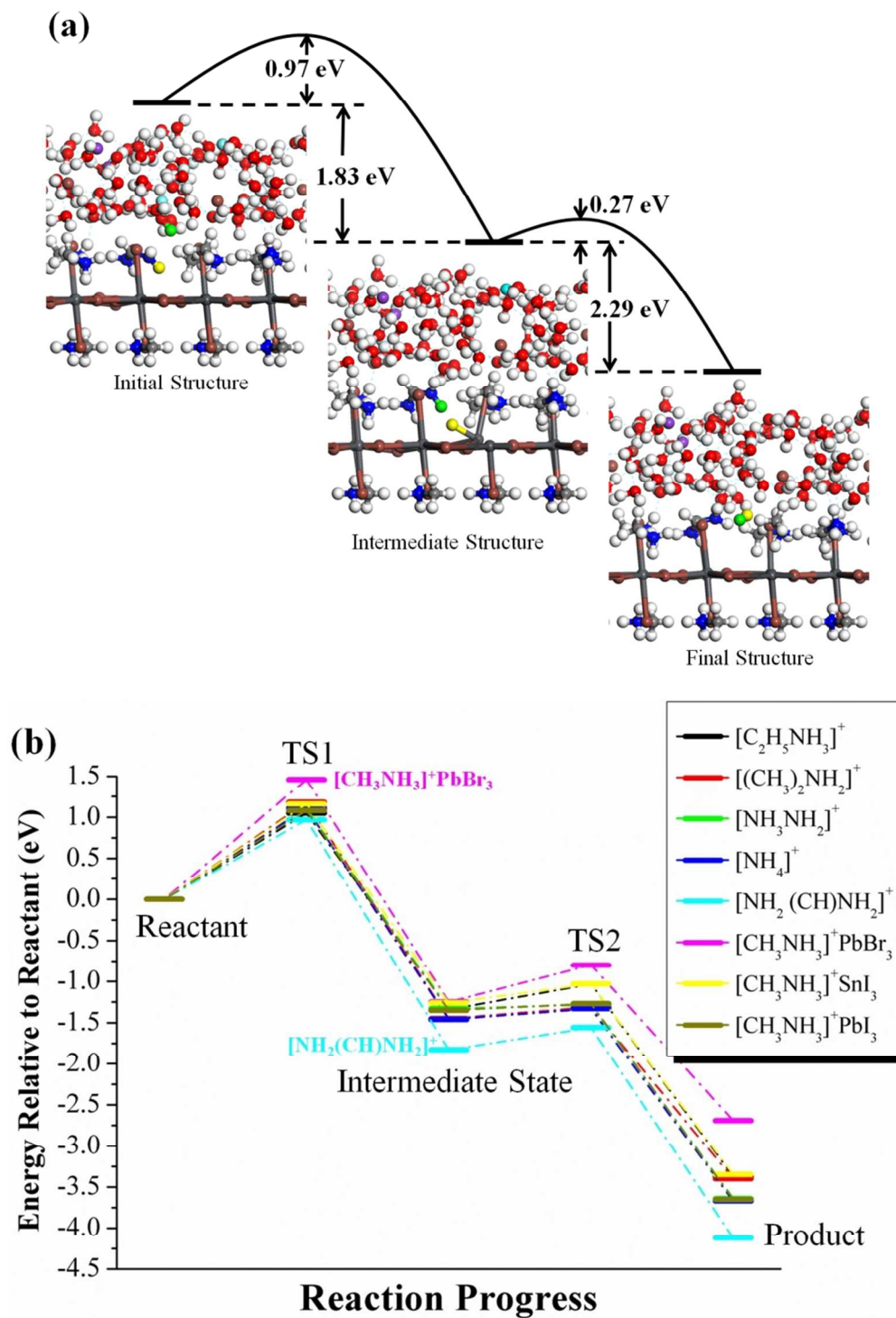


Figure 2. (a) The reaction pathway for H₂ generation at the NH₂(CH)NH₂⁺ site on the CH₃NH₃PbI₃ surface in acidic solution; (b) the energetics (relative to reactant) for various organic-inorganic hybrid perovskites. The green and the yellow balls indicate two H from NH₂(CH)NH₂⁺ to form H₂, and the cyan color indicates two protons in the solution that involved in the Grotthuss chains.